View metadata, citation and similar papers at core.ac.uk

brought to you by CORE

provided by Elsevier - Publisher Connector

Biochimica et Biophysica Acta 1808 (2011) 1544–1551

Contents lists available at ScienceDirect

Biochimica et Biophysica Acta

journal homepage: www.elsevier.com/locate/bbamem

Retro-inversion of certain cell-penetrating peptides causes severe cellular toxicity

Tina Holm [a,*,1], Helin Räägel [b,1], Samir EL Andaloussi [a], Margot Hein [b], Maarja Mäe [a], Margus Pooga [b], Ülo Langel [a]

[a] Department of Neurochemistry, Stockholm University, SE-106 91 Stockholm, Sweden
[b] Institute of Molecular and Cell Biology, University of Tartu, 510 10 Tartu, Estonia

ARTICLE INFO

Article history:
Received 3 August 2010
Received in revised form 5 October 2010
Accepted 29 October 2010
Available online 9 November 2010

Keywords:
Cell-penetrating peptide
Retro-inverso
Cytotoxicity
Hydrophobicity
Apoptosis

ABSTRACT

Cell-penetrating peptides (CPPs) are a promising group of delivery vectors for various therapeutic agents but their application is often hampered by poor stability in the presence of serum. Different strategies to improve peptide stability have been exploited, one of them being "retro-inversion" (RI) of natural peptides. With this approach the stability of CPPs has been increased, thereby making them more efficient transporters. Several RI-CPPs were here assessed and compared to the corresponding parent peptides in different cell-lines. Surprisingly, treatment of cells with these peptides induced trypsin insensitivity and rapid severe toxicity in contrast to L-peptides. This was measured as reduced metabolic activity and condensed cell nuclei, in parity with the apoptosis inducing agent staurosporine. Furthermore, effects on mitochondrial network, focal adhesions, actin cytoskeleton and caspase-3 activation were analyzed and adverse effects were evident at 20 μM peptide concentration within 4 h while parent L-peptides had negligible effects. To our knowledge this is the first time RI peptides are reported to cause cellular toxicity, displayed by decreased metabolic activity, morphological changes and induction of apoptosis. Considering the wide range of research areas that involves the use of RI-peptides, this finding is of major importance and needs to be taken under consideration in applications of RI-peptides.

© 2010 Elsevier B.V. All rights reserved.

1. Introduction

Cell-penetrating peptides (CPPs) are relatively short, cationic and/or amphipathic peptides that have successfully been exploited to convey a wide range of cargos into different cell-lines *in vitro*, as well as *in vivo*. The major advantages associated with this class of delivery vectors, apart from their high delivery efficacy, is that they generally display low toxicity and that there appear to be no size restraints in terms of cargo compounds that can be transported into cells using these peptides [1]. One shortcoming, however, that has been realized in the last few years, is the frequent accumulation of CPPs in the endosomal compartments, which greatly reduces the bioavailability of the cargo molecules. Several different strategies have successfully been explored to overcome this problem, either by introducing chemical modifications in CPPs or by conjugating fusogenic peptides to CPPs [2,3]. Another major issue that needs to be addressed is the rapid degradation of CPPs in the presence of serum. Almost all naturally occurring polypeptides are composed of L-amino acids and, consequently, the cellular proteolytic machinery does not recognize D-amino acids. Thus, substituting L- with D-amino acids in a peptide sequence increases its stability. This approach has proven successful for several CPPs, e.g. polyarginine, pVEC, and penetratin [4,36,5]. However, this conversion yields peptides which are enantiomers and, thus, the stereochemistry is not the same. Although making polyarginine and pVEC more stable and thereby more efficient transporters, the stereochemistry might be important for other CPPs. Furthermore, this modification is not suitable when the topology of the peptide is essential for activity.

In the early 1980s, Chorev and Goodman carried out extensive research on the chemistry of peptide backbone modifications [6]. They hypothesized that exchanging a natural peptide sequence with all-D amino acids (inverso) and reversing the order (retro) would yield a peptide with the same stereochemistry as the parent peptide. These peptidomimetics were named retro inverso (RI) peptides, where the side groups are oriented in the same way, but the amine and carbonyl of the amide peptide bond are reversed. In an extensive review from 2005, Chorev [7] presents a number of successful implementations of the RI concept. However, RI modification of natural peptides has a history of mixed success and several groups have reported that their RI-peptides lost the biological activity of the parent L-peptide [8,9]. Also CPPs have been subjected to this modification, with the aim of producing transporters with increased stability. To our knowledge the

Abbreviations: CPP, cell-penetrating peptide; RI, retro inverso; PNA, peptide nucleic acid; PI, propidium iodide; LDH, lactate dehydrogenase; FA, focal adhesion

* Corresponding author. Stockholm University, S.Arrheniusv. 21A, SE-106 91 Stockholm, Sweden. Tel.: +46 8 164266; fax: +46 8 161371.
E-mail address: tina@neurochem.su.se (T. Holm).

[1] These authors contributed equally to this work.

0005-2736/$ – see front matter © 2010 Elsevier B.V. All rights reserved.
doi:10.1016/j.bbamem.2010.10.019

only CPPs reported in the literature to have increased activity in their RI forms are the frequently used Tat [10] and penetratin peptides [11].

The aim of our study was to increase the stability of a CPP (M918) designed in our lab, thereby making it a more potent transporter [12]. Another CPP (p14Arf), previously reported by our group to have apoptogenic effects was also subjected to the RI modification in order to enhance its efficacy [13]. The two most commonly used CPPs Tat and penetratin were studied in RI mode for comparison. The results indicate that cytotoxicity arises with RI-peptides above a certain length. Also the high number of hydrophobic amino acids in the peptide sequence might have a role in the induction of toxicity.

2. Materials and methods

2.1. Peptide synthesis

Peptides with either L- or D-amino acids, PNA and peptide-PNA conjugates were synthesized with *t*-Boc chemistry as described in [13].

2.2. Cell culture

MCF-7 and MDA MB 231 (human breast cancer cell lines) cells (ATCC) were cultured in RPMI-1640 medium supplemented with FBS (10%), penicillin (100 U ml^{-1}), streptomycin (100 μg ml^{-1}), sodium pyruvate (1 mM), and non-essential amino acids (1%). HeLa pLuc 705 cells, kindly provided by R. Kole, were cultured in DMEM with glutamax, using the same supplements as above. HeLa cells were cultured in IMDM medium supplemented with FBS (10%), penicillin (100 U ml^{-1}) and streptomycin (100 μg ml^{-1}). All cells were grown at 37 °C and 5% CO_2 and all cell culture material were purchased from Invitrogen.

2.3. Cell proliferation assay

Cell proliferation was studied with the Roche Wst-1 proliferation assay according to the manufacturer's instructions (Roche Diagnostics Scandinavia AB, Sweden). Briefly, cells were seeded in 96 well plates 2 days prior the experiment to reach 80% confluency. Peptides were added at different concentrations in RPMI or IMDM medium (100 μl) followed by incubation for 4 h. The peptide solution was removed, fresh medium added and the incubation was continued for another 20 h. Wst-1 substrate (10 μl) (Roche) was added to every well and after 1–4 h absorbance was measured (450 nm) using Digiscan absorbance reader (Labvision via AH Diagnostics AB, Sweden). The percentage of viable cells was determined using GraphPad Prism software 4.0 (GraphPad Software, CA).

2.4. Membrane integrity assay

Membrane integrity was assessed using the Promega CytoTox ONE assay (Promega, Sweden). In brief, cells were seeded in 96-well plates two days prior the experiment to reach 80% confluency. Peptides were added at different concentrations in Hepes Krebs Ringer (HKR) (100 μl) and after 30 min incubation the exposure solution was transferred to a 96-well black plate, followed by addition of the CytoTox-ONE™ reagent. The plate was incubated for 10 min at RT and then fluorescence was measured (560/590 nm) with SPECTRAmax® GEMINI XS spectrofluorometric plate reader (Molecular Devices, USA). The results are presented as percentage of the maximum LDH release (100%) from 0.18% Triton X-100 treated cells.

2.5. Splice correction

60 000 HeLa pLuc 705 cells/well were seeded in 24-well plates. After 24 h, medium was removed and cells were overlaid with CPP-PNA conjugates at different concentrations in 500 μl optiMEM® reduced serum media (Invitrogen). Cells were incubated for 4 h whereafter 1 ml of full growth medium was added to each well. After an additional 20 h, medium was removed and cells were washed twice with HKR and subsequently lysed using 100 μl of 0.1% Triton X-100 in HKR. After 30 min incubation on ice, 20 μl cell lysates were transferred to white 96-well plates. Luciferase activity in cell lysates was measured on a Flexstation II (Molecular Devices, USA) using the Promega luciferase assay system according to manufacturers protocol (Promega) and normalized to protein content.

2.6. Fluorescence microscopy on fixed cells

35 000 HeLa or MDA MB 231 cells/well were seeded onto glass coverslips (Ø 12 mm, Marienfeld Superior, Germany) in 24-well plates 2 days before experiment. On the day of experiment, cells were washed, incubated with 10 or 20 μM peptides for 4 h in serum free IMDM or RPMI medium at 37 °C (for negative control, cells were incubated 4 h in medium without peptides), washed again and fixed with 4% paraformaldehyde (PFA) in PBS on ice for 30 min. Permeabilization of cells was performed with 0.1% Triton X-100 in PBS on ice for 5 min, cells were then blocked with 10% non-fat dry milk (NFDM) in PBS for 30 min and incubated with either 8.5 μg ml^{-1} rabbit polyclonal antibody to zyxin (for staining of focal adhesions) (ab11518, Abcam, UK) in 1% NFDM in PBS for 1.5 h and 10 μg ml^{-1} goat-anti-rabbit-Alexa-594 (Molecular Probes, OR) in 1% NFDM in PBS for 1 h or with 0.4 U ml^{-1} phalloidin-Alexa-488 (Molecular Probes, OR) in 1% NFDM in PBS. As positive control for actin polymerization, cellular actin fibers were induced with 5 μM lysophosphatidic acid (LPA) for 15 min, following the above described protocol for cell fixation and actin visualization. Cells were mounted with either 30% glycerol in PBS or Fluoromount (Sigma, MO) and visualized by Olympus FV1000 confocal microscopy (zyxin/focal adhesions) or Olympus BX61 microscope equipped with a CCD camera DP70 (phalloidin/actin). For visualization of caspase-3, cells were incubated with 20 μM penetratin, RI-penetratin, Arf1-14 or RI-Arf1-14, or 50 μM RI-penetratin or RI-short penetratin as described above, afterwards fixed and stained for caspase-3 according to the manufacturer's protocol (R&D Systems, Inc., MN). Briefly, treated cells were fixed with freshly made 4% PFA in PBS for 30 min on ice, incubated with 1 μg ml^{-1} rabbit polyclonal caspase-3 antibody in PBS containing 1% BSA, 1% goat serum and 0.3% Triton X-100 for 30 min in a humidified chamber. Cells were then incubated with goat anti-rabbit-Alexa-594 secondary antibody (Molecular Probes, OR) (1:250 dilution in 1% BSA in PBS) for 30 min. Additionally, DAPI staining (0.5 μg ml^{-1}) was performed. Cells were mounted to 30% glycerol in PBS and imaged by Olympus FV1000 confocal microscope.

2.7. Fluorescence microscopy on live cells

8000 HeLa or MDA MB 231 cells/well were seeded onto 8-chambered cover glasses (Nalge Nunc International, NY) 2 days before experiment. Cells were incubated with 10 or 20 μM long RI- and L-peptides, or 50 μM RI-short penetratin for either 3 h (MDA MB 231), visualized immediately after adding the peptides for 0–45 min (timelapse) or pulsed for 4 h and chased for additional 20 h (HeLa) at 37 °C. 45 min prior to visualization, 10 nM MitoTracker (M7512, Molecular Probes, OR) was added. Cells were imaged using an Olympus FV1000 confocal microscope and images were analyzed with Olympus FV10 ASW software version 1.6.

2.8. Hoechst staining

Cells were seeded on cover slips in 24-well plates two days before the experiment, to reach a confluency of 70–80% on the day of the experiment. Peptides were added at different concentrations in RPMI

medium and incubated for 4 h. The peptide solution was removed, fresh medium added and incubation continued for another 20 h. The coverslips were washed, fixed with 4% PFA, stained with Hoechst 33342 for 5 min at RT, washed, mounted on glass slides, and then analyzed by fluorescence microscopy (Leica DMIRE2 fluorescence microscope). Quantification of the cell images (n>400 for each treatment) was done by counting the number of condensed and normal nuclei, then calculating the percentage of condensed nuclei and normalizing it against staurosporine treated cells.

3. Results

3.1. Cellular translocation of fluoresceinyl-labeled RI-CPPs

Five RI-peptides and their normal counterparts composed of L-amino acids were synthesized and evaluated in this study (Table 1). To establish that the peptides retained their cell-penetrating ability after RI-isomerization, they were all labeled N-terminally with fluorescein and cellular uptake was confirmed with confocal microscopy. Within 30 min at 5 μM concentration, all peptides displayed a vesicular-like uptake pattern (data not shown).

3.2. Retro inversion of CPP does not confer increased cellular internalization

M918 is an efficient CPP recently discovered by EL Andaloussi et al. [12]. This peptide is capable of delivering various cargos including plasmids, proteins and oligonucleotides into a wide range of cell-lines. With the aim of making this CPP more stable, and thereby possibly more efficient, we synthesized its retro-inverso analogue. The splice correction assay has become a powerful method in evaluation of the delivery properties of CPPs since it generates a biological positive read-out (for a detailed description of the method, see [14,15]). This assay makes use of HeLa cells that are stably transfected with a luciferase reporter gene that is interrupted by a thalassemic intron carrying an aberrant splice site [15]. Under normal conditions, these HeLa pLuc 705 cells will produce luciferase transcripts carrying parts of the intron and concomitantly non-functional luciferase protein is produced. However, if a steric block splice-correcting oligonucleotide that binds complementary to the mutated position is introduced to the nucleus of cells, splicing will be re-directed and functional luciferase produced. Thus, by covalently conjugating RI-M918 to splice correcting antisense peptide nucleic acid (PNA) oligomer (Table 1) the delivery properties could be assessed by measuring the increase in luminescence. Surprisingly, RI-M918-PNA was not significantly better than M918-PNA at inducing splice correction at 2 and 5 μM, and at 10 μM correction was abolished when using RI-M918 whereas the parent M918-PNA promoted a further increase in splice correction (Fig. 1). The drop in luminescence at 10 μM RI-M918 suggests that the cells are not viable and unable to produce luciferase.

Table 1
Names and sequences of the peptides and PNA used in the study.

Name	Sequence
Arf 1-14	MVRRFLVTLRIRRA-amide
RI-Arf 1-14	arrirltvlfrrvm-amide
RI-Arf1-14 inv	arrirlrrflvtvm-amide
M918	MVTVLFRRLRIRRASGPPRVRV-amide
RI-M918	vrvrppgsarrirlrrflvtvm-amide
Penetratin	RQIKIWFQNRRMKWKK-amide
RI-penetratin	kkwkmrrnqfwikiqr-amide
Tat	YGRKKRRQRRR-amide
RI-Tat	rrrqrrkkrgy-amide
RI-short penetratin	nqfwikiqr-amide
M705 PNA	CysKK**CCTCTTACCTCAGTTACA**KK-amide

Peptides are fluoresceinyl-labeled on the N-terminus. Lower case letters indicate D-amino acids. Bold letters represent nucleobases. For the formation of conjugates, M918 and RI-M918 were synthesized with N-terminal Cys(Npys). Conjugates are illustrated as follows: CPPCys-S-S-CysPNA and abbreviated, e.g. M918-PNA.

3.3. RI-CPPs reduce the viability of cells

All peptides (Table 1) were assessed using the Wst-1 assay to determine their impact on cell viability. In our previous publication on the use of the p14Arf peptide [13] (from now on called Arf1-14), two different breast cancer cell-lines were used; MDA MB 231 and MCF-7. In order to compare the effects of RI-Arf1-14 and its parent peptide, the same cells were used and, in addition, the effect on HeLa cells was investigated, since this is one of the most commonly used cell-line. Staurosporine, an apoptosis-inducing agent, was included as control. None of the control peptides composed of L-amino acids reduced the viability of cells, and every RI-peptide was normalized against its L-peptide counterpart. In keeping with the results from the splice correction assay, RI-M918 reduced the cellular viability by 30% in HeLa cells at 10 μM (Supplementary Fig. S1b), and the effect was even more pronounced in the other cell-lines (50-70% reduction) (Fig. 2 and Supplementary Fig. S1a). RI-Tat and RI-short penetratin were not toxic in the tested concentration range. However, full length RI-penetratin (RI-penetratin) had a dramatic effect on cellular viability. At 10 μM, it reduced the viability by 75% in MDA MB 231 cells (Fig. 2). This is remarkable since staurosporine only reduced viability by 50%. The effect of RI-Arf1-14 was similar in both MDA MB 231 and MCF-7 cells, with 40–50% reduced viability at 10 μM concentration and 80–90% reduced viability at 20 μM (Fig. 2 and Supplementary Fig. S1a). HeLa cells are more robust and although significant reduction in viability was observed, none of the RI-peptides reduced the viability by more than 50% (Supplementary Fig. S1b).

To rule out that the observed toxic effects were due to extensive membrane damage after peptide treatment, leakage of lactate dehydrogenase (LDH) was measured. None of the peptides caused leakage above 8% in any of the tested cell-lines up to 20 μM concentration (Supplementary Fig. S2a–c).

3.4. RI-CPPs induce trypsin insensitivity of treated cells

The amount of apoptotic cells was initially assessed by the Annexin V assay. Surprisingly, cells treated with RI-CPPs did not detach from the plastic neither with enzymatic trypsin treatment nor with EDTA. The possibility of RI-peptides inhibiting the trypsin activity was assessed and no interference with its enzymatic activity was observed for any of the RI-peptides (data not shown). Therefore, to visualize the morphological changes in cells after RI-CPP treatment, MDA MB 231 and HeLa cells were incubated with 20 μM penetratin, RI-penetratin,

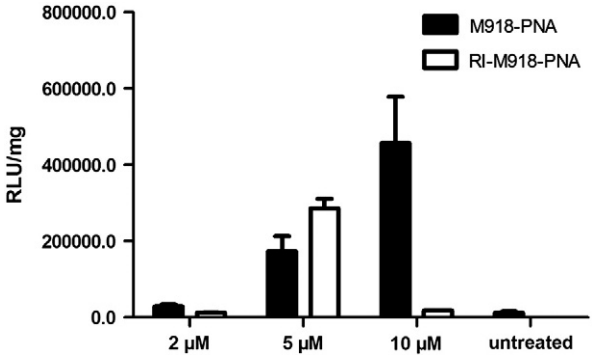

Fig. 1. Retro inversion of the CPP does not confer increased cellular internalization. Splice correction was measured 24 h after treatment with CPP-PNA conjugates at the indicated concentrations. Light emission (RLU) is normalized to the protein content in each well and data presented as RLU/mg. Depicted are mean and standard error of the mean (SEM) of triplicate results that are representative of multiple experiments.

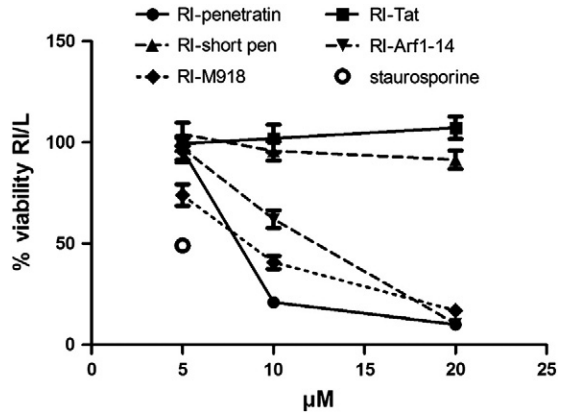

Fig. 2. RI-CPPs reduce the viability of cells. Cell viability of MDA MB 231 cells was determined by measuring their metabolic activity with the Wst-1 assay. Cells were treated with peptides at indicated concentrations for 4 h. The peptide solution was then removed, fresh medium added, and cells were incubated for another 20 h. Staurosporine (0.5 μM) was included as positive control. The effect of RI-peptides on viability was normalized against the effect of their L-peptide counterpart. Mean and standard error of the mean (SEM) of multiple experiments are depicted.

M918, RI-M918, Arf1-14 or RI-Arf1-14 for 4 h at 37 °C. Subsequently, trypsin treatment was carried out to observe cell rounding effects using confocal microscopy where time-lapse images were taken after every 15 s (Supplementary Fig. S3a–h and Supplementary movies M1).

M918, penetratin and Arf1-14 did not alter the phenotypic appearance of the cells and during trypsin treatment, all the cells turned spherical within 2–5 min (Supplementary Fig. S3a, c, e and g, Supplementary movie M1 a, c, e and g, and data not shown). Additionally, propidium iodide (PI), which is impermeable to cells with intact membranes, did not stain any of the visualized cells. RI-M918 (data not shown), RI-Arf1-14 and RI-penetratin, on the other hand, generated a remarkable change in the morphology of MDA MB 231 cells with a strongly granulated cytoplasm, a blebbing plasma membrane and a risen/mispositioned nucleus (Supplementary Fig. S3b and d. Supplementary movie M1, b and d). When applying trypsin, we observed no movement or rounding of cells even after 15 min. RI-CPPs clearly exerted a cytotoxic effect on the cells detected as severe morphological alterations and strong intracellular PI signal.

3.5. RI-CPPs prohibit formation of focal adhesions and induce disassembly of the actin cytoskeleton

Since trypsin had no effect on cells treated with RI-CPPs and that cells were firmly attached to the plastic even after longer enzymatic treatment, we investigated the condition of focal adhesions (FAs) in cells possessing the risen nucleus phenotype. For that, HeLa cells were incubated with 10 (Supplementary Fig. S4) or 20 μM (Fig. 3) penetratin, RI-penetratin, Arf1-14 or RI-Arf1-14 for 4 h at 37 °C and focal adhesion protein zyxin was visualized by immunofluorescence and microscopic analysis.

FAs in penetratin- and Arf1-14-treated cells were similar to control cells, where zyxin was located in short and relatively thick bundles (Fig. 3 and supplemental Fig. S4). RI-penetratin, induced the formation of longer and thinner adhesive structures, especially when lower concentration (10 μM) was used.

RI-Arf1-14-treatment (20 μM) led to the disappearance of all FAs in cells possessing the risen nucleus phenotype (Fig. 3). In the few cells (about 5%) still forming observable FAs after 10 μM RI-Arf1-14 treatment, the FAs were similar to those found in RI-penetratin treated cells with an extended and thinner appearance (Supplementary Fig. S4).

The actin filaments, as one of the cellular cytoskeletal components responsible for cell stretching, adhesion and intracellular mechanical tension, terminate with focal adhesions at the cell membrane [16]. Since drastic alterations in adhesive structures were observed in RI-CPP-treated cells, we next analyzed the intactness of the actin cytoskeleton in MDA MB 231 and HeLa cells after treatment with 20 μM peptides for 4 h by visualizing the polymerized actin with the phalloidin-staining.

In MDA MB 231 cells, both RI-penetratin and RI-Arf1-14 dissociated the central actin filaments, leading to a diffuse unorganized localization of actin (Fig. 4). The cortical actin fibers were, however, present in most of the RI-penetratin-treated cells. In contrast, when using RI-Arf1-14, the cortical actin bundles were missing in approximately 80–90% of cells. Additionally, the induction of filopodia-like structures was observed in RI-peptide-treated cells, especially with RI-Arf1-14, where the membrane area was undulating more as a result of the loss of stabilizing cortical actin. The L-counterpart peptides did not affect the cells and the actin skeleton was similar to control cells.

In HeLa cells, RI-penetratin-treatment destroyed most of the central actin filaments and led to the formation of large flat areas lined with numerous filopodia-like structures (Supplementary Fig. S5). RI-Arf1-14 affected both types of actin filaments, disassembling the cortical along with the central actin cables. Corroborating the results in MDA MB 231 cells, HeLa cells treated with penetratin and Arf1-14 did not appear different from the control cells.

3.6. RI-CPPs disrupt the mitochondrial network and induce apoptosis

In light of the extreme morphological and cytotoxic effects of the studied RI-peptides, we examined the integrity of the mitochondrial network in MDA MB 231 and HeLa cells using MitoTracker as a marker for active mitochondria. During early apoptotic events the inner mitochondrial transmembrane potential is disrupted [17], leading to a decreased signal from the MitoTracker probe.

The L-peptides did not affect the mitochondrial potential neither in MDA MB 231 (Fig. 5) nor in HeLa cells (Supplementary Fig. S6). RI-

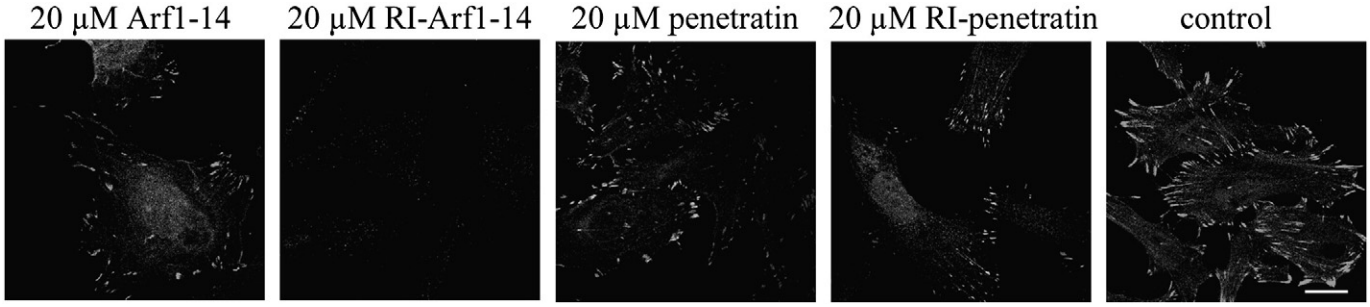

Fig. 3. RI-CPPs prohibit the formation of focal adhesions. Focal adhesions in HeLa cells were visualized with anti-zyxin antibody after peptide treatment. Cells were incubated with 20 μM Arf1-14, RI-Arf1-14, penetratin or RI-penetratin for 4 h. Control cells were incubated in IMDM medium without peptides. Bar 10 μm.

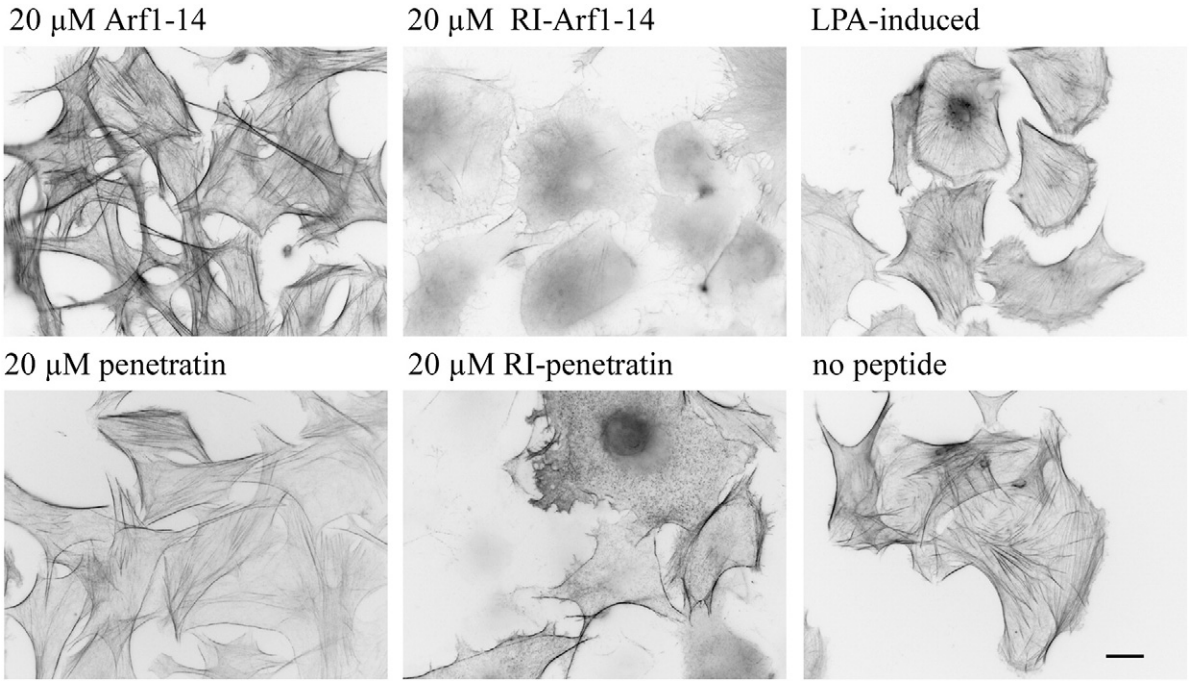

Fig. 4. RI-CPPs induce disassembly of the actin cytoskeleton. MDA MB 231 cells were treated with 20 μM penetratin, RI-penetratin, Arf1-14 or RI-Arf1-14 for 4 h. Cellular actin fibers were induced with 5 μM lysophosphatidic acid (LPA) for 15 min as positive control for actin polymerization (upper right panel). Untreated cells incubated in RPMI medium are shown in the lower right panel (no peptide). The actin cytoskeleton was visualized with phalloidin-Alexa-488. Image has been color-inverted for better visualization of actin filaments. Bar 10 μm.

peptides, on the other hand, exhibited a detrimental effect on the mitochondrial network already after 3 h, especially in MDA MB 231 cells (Fig. 5). RI-penetratin-treatment caused disruption of the mitochondrial network in about 50% and RI-Arf1-14 in more than 95% of cells. In HeLa cells, RI-Arf1-14-treatment completely abolished the mitochondrial network. RI-penetratin had a much milder impact on HeLa cells and the mitochondrial network was still apparent (supplemental Fig. S6). The short penetratin analogue RI-short penetratin did not cause any visible discrepancies in the mitochondrial network compared to the untreated cells even at higher concentrations (50 μM) (Fig. 5).

We also analyzed the effect of RI-Arf1-14 on the mitochondria in a time dependent manner and detected the first variations in mitochondrial signals already after 15–20 min (supplemental movie M2). The gaps in the network grew larger until completely disappearing after 45 min–1 h incubation. Along with the loss of mitochondrial signal, the cells underwent the morphological changes described above.

The observed nuclear changes and the possible involvement of apoptosis were further investigated by Hoechst staining of condensed nuclei. Cells treated with peptides, or staurosporine, were stained with Hoechst nuclear dye and analyzed by fluorescence microscopy. The L-peptides (M918, Arf1-14, penetratin and Tat) did not induce changes in nuclear morphology, while the RI-peptides (RI-M918, RI-Arf1-14 and RI-penetratin) induced chromatin condensation comparable with, or higher than, staurosporine. Cells treated with L-peptides or RI-Tat and RI-short penetratin displayed condensed nuclei in the same range as the untreated cells (Fig. 6).

3.7. RI-CPPs activate caspase-3

During apoptosis, several cellular caspases, e.g. caspase-3, are crucial mediators for inducing the programmed cell death [18]. Since the aforementioned alterations in cell viability, morphology, attachment and mitochondria refer to the induction of apoptosis, we studied the caspase-3 activation in MDA MB 231 and HeLa cells. The cells were treated with 20 μM penetratin, RI-penetratin, Arf1-14 or RI-Arf1-14, or 50 μM RI-penetratin and RI-short penetratin for 4 h. We observed a significant induction of caspase-3 activation in response to RI-Arf1-14-treatment in both cell lines (MDA MB 231 (Fig. 7) and HeLa (Supplementary Fig. S7)). Surprisingly, RI-penetratin did not induce activation of caspase-3 at 20 μM concentration, although slightly

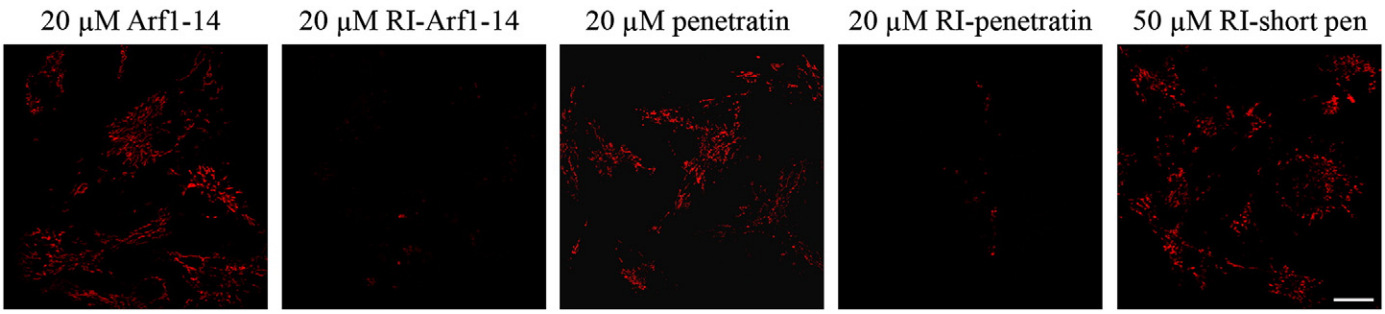

Fig. 5. Longer RI-peptides disrupt the mitochondrial network. The mitochondrial network in MDA MB 231 cells was labeled with MitoTracker 45 min prior to visualization with confocal microscopy. Cells were incubated with 20 μM penetratin, RI-penetratin, Arf1-14 or RI-Arf1-14, or with 50 μM RI-short penetratin (RI-short pen) for 3 h. Bar 10 μm.

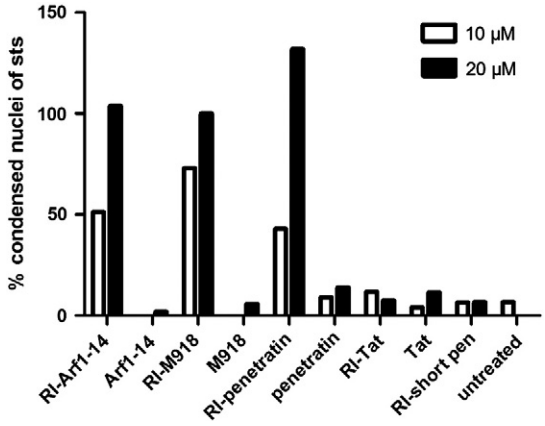

Fig. 6. RI-CPPs induce nuclear condensation. MCF-7 cells were incubated with peptides at 10 or 20 μM concentration for 4 h. The peptide solution was then removed, fresh medium added, and the cells were incubated for another 20 h. Cell nuclei were stained with Hoechst nuclear dye and analyzed with fluorescence microscopy. Quantification was done by counting the number of normal nuclei and nuclei with condensed chromatin for each concentration (at least 400 cells). Results are presented as percent of condensed nuclei normalized to 0.5 μM staurosporine (sts) treated cells.

stronger fluorescence signal was detected in RI-penetratin-treated cells as compared to control or L-peptide-treated cells. However, increasing the concentration of RI-penetratin to 50 μM resulted in similar activation of caspase-3 as in RI-Arf1-14-treated cells. Similar effect was seen with RI-M918, where a higher concentration (50 μM) of the peptide was needed to induce caspase-3 activation (data not shown). On the other hand, neither RI-short penetratin (Fig. 7) nor RI-Tat (data not shown) affected caspase-3 activation even at higher concentrations.

4. Discussion

The stability of the potent transport vectors called cell-penetrating peptides (CPPs) in the presence of serum or blood plasma has emerged as one of the limiting steps in their successful application *in vivo* [19]. To increase the peptide's resistance to premature degradation or proteolysis, several methods have been used, including D-isomerization and retro-inversion (RI) techniques. With the aim of improving the stability of a novel CPP called M918 displaying improved transporting abilities in different cell-lines [12], we synthesized its RI counterpart. When assessing the transport efficiency of M918 and its RI-isoform, we unpredictably found that cells treated with RI-M918-PNA displayed drastic morphological changes, indicative of cytotoxicity.

Another effective CPP p14Arf, which has been shown to induce apoptosis, [13] was subjected to the RI isomerization. However, since it has been reported that the N-terminal 14 amino acids of p14Arf are sufficient for peptide activity [20], we made p14Arf 1-14 in RI mode. As a control peptide, p14Arf1-14 with L-amino acids was synthesized. The initial results were promising since the cell-penetrating capability was retained and Wst-1 data showed that RI-Arf1-14 reduced the viability of MDA MB 231 and MCF-7 cells by 50% at 10 μM concentration (Fig. 2 and Supplementary Fig. S1a), without causing leakage of LDH (Supplementary Fig. S2). However, to ascertain that the reduced viability was not due to unspecific toxicity, but indeed due to the interaction of RI-Arf1-14 peptide with its target protein [13], a control peptide was synthesized, where the five amino acids crucial for target interaction were inverted, producing a peptide with no effect on cell viability. Unexpectedly, this peptide caused an analogous reduction in cell viability as RI-Arf1-14 (data not shown), suggesting that the reduced proliferation was not due to RI-Arf1-14 *per se*, but more likely as a result of the RI modification of the peptide. In order to verify our findings, two widely used CPPs–Tat and penetratin–were synthesized in the RI-mode and analyzed for cytotoxicity. RI-penetratin was found to be as cytotoxic as RI-Arf1-14 and RI-M918, as determined with the Wst-1 assay (Fig. 2), while RI-Tat did not affect the cells at all. In addition, we also found that cells treated with RI-Arf1-14, RI-M918 and RI-penetratin, could not be detached from the cell culture plates, neither with trypsin nor with EDTA. This observation, together with the results from splice correction and Wst-1 assays, were the first indications that RI-peptides might cause adverse cellular effects and it prompted us to investigate this phenomenon further.

Treatment of both MDA MB 231 and HeLa cells with RI-penetratin and RI-Arf1-14 induced extensive alterations in cell morphology. As depicted in Fig. 3 and 4, the mechanism(s) behind these alterations may lie in the structural changes of the actin cytoskeleton and concomitantly the focal adhesions due to treatment with the RI-peptides. Since some CPPs have been demonstrated to directly interact with the monomeric actin [21], they could, as a result, also interfere with the polymerization or rearrangement processes causing the above mentioned effects. Moreover, due to the increased stability of the RI-peptides, their effects inside the cells could be amplified by several fold because of their lack of removal by the cell's proteolytic machinery. Additionally, the actin cytoskeleton and its remodeling plays a crucial role in many cellular processes, i.e. cell spreading, adhesion, contraction, etc. [22] and, therefore, its disruption or depolymerization may lead to inhibition of cellular events resulting in abnormal functioning of the cell. For example, it has been shown that the actin cytoskeleton is involved in the cortical retraction of mitotic cells and in case of its disruption by inhibition of upstream effectors (i.e. RhoA and Rho-kinase/ROCK), the cells undergoing mitosis do not turn spherical [23]. Similar outcome was observed in our trypsin-treatment experiments, where cells without the presence of actin filaments did not obtain a globular form. Also, the risen nucleus of RI-peptide-treated cells is possibly caused by the disassembly of the actin skeleton since actin filaments are essential for nuclear positioning and anchorage [24]. Furthermore, it has been shown that actin disruption may evoke apoptosis [25], affirming the damage that some of the RI-peptides cause the cells.

Adverse toxic effects were observed for all the RI-peptides, except for RI-Tat. Since RI-Tat is only 11 amino acids long, we hypothesized that this could be one of the reasons for the observed difference in toxicity of the RI-peptides. We therefore synthesized a truncated version of RI-penetratin with only the first 9 amino acids, named RI-short penetratin. This peptide was also nontoxic to the cells, suggesting that RI-peptides above a certain length cause these adverse effects. The importance of the peptide length on the cytotoxicity has been demonstrated before for e. g. polyarginine [26]. The length of the peptide may determine, for example, the depth of membrane insertion, since it has been demonstrated with Transportan (TP) [27], that the longer peptides are capable of spanning the whole lipid bilayer, whilst shorter peptides can submerge only to the outer membrane leaflet. Additionally, the shortening of MAP peptide by four amino acid residues either N- or C-terminally (corresponding to the removal of one of the α-helix turns), eliminated its toxic effects [28]. The results on MAP indicate that there may be a correlation between helicity (a membrane interacting secondary structure) and cytotoxicity. We therefore hypothesize further that the ability to form secondary helical structure is important for efficient internalization but might also cause toxicity. Grounds for such hypothesis comes from the notion that all the toxic peptides used in this study–RI-Arf1-14, RI-penetratin, and RI-M918–contain amino acids that are frequently found within helices, e. g. alifatic amino acids, whereas RI-Tat is mostly composed of cationic residues that are less likely to form a helix. Also, both RI-Tat and RI-short penetratin are likely too short to form a secondary structure. Furthermore, as demonstrated by EL Andaloussi et al [29], the quantitative uptake of Tat is about 50 times lower than penetratin

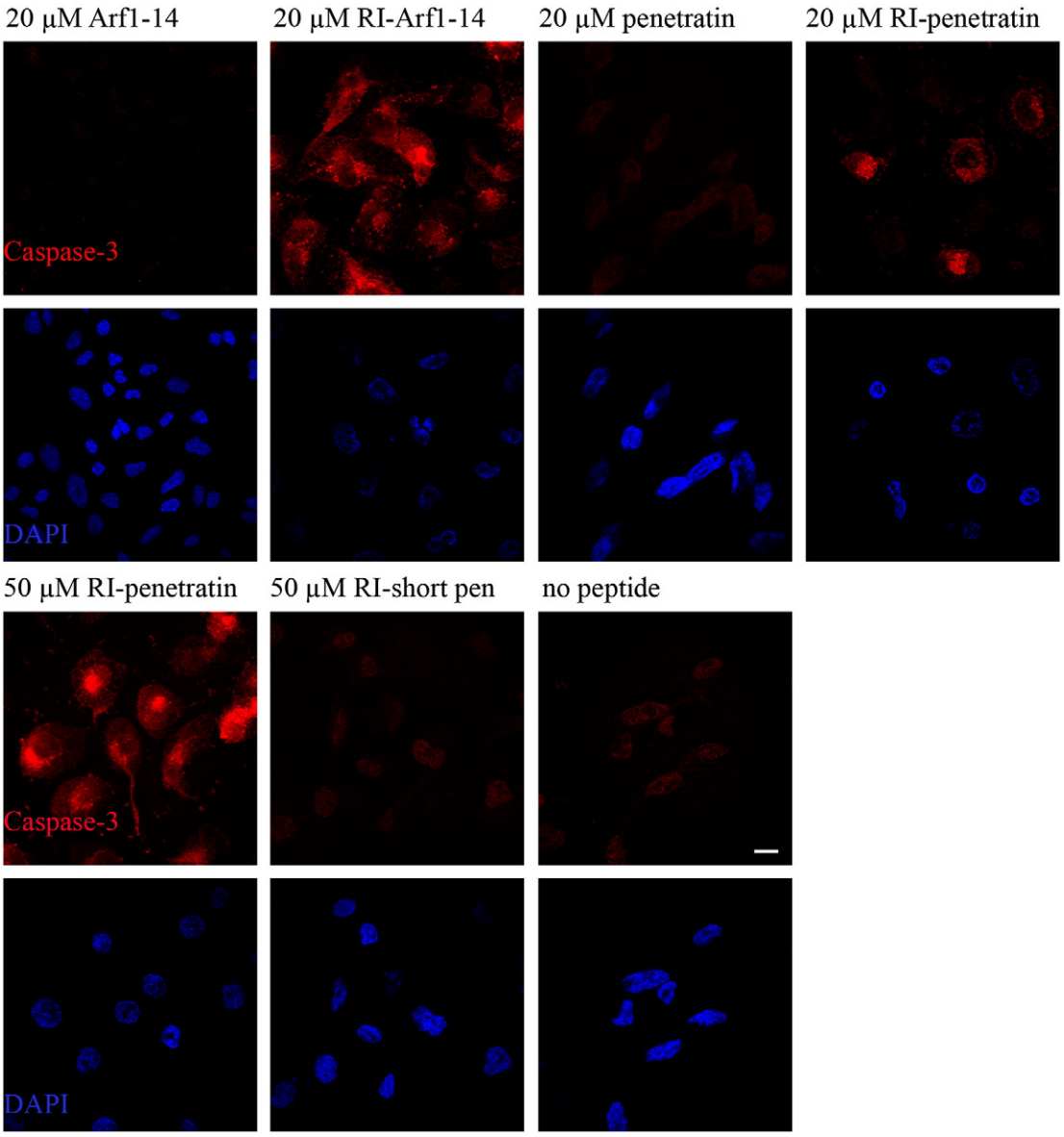

Fig. 7. RI-Arf1-14 (20 μM) and RI-penetratin (50 μM) induce activation of caspase-3. Caspase-3 antibody with the secondary Alexa594-conjugated antibody was used to visualize activation of caspase-3 after peptide treatment. MDA MB 231 cells were incubated with 20 μM Arf1-14, RI-Arf1-14, penetratin, RI-penetratin or 50 μM RI-penetratin or 9-mer RI-short penetratin (here RI-short pen) for 4 h. Lower panels show DAPI stained cells. Control cells were incubated in RPMI medium without the peptides (no peptide). Bar 10 μm.

at 5 μM, corroborating the result of many different groups that Tat peptide per se is not very potent in entering cells [30–32]. Therefore, the difference in toxicity displayed by the short versus the longer RI-peptides may additionally be due to higher intracellular levels of the latter.

Put together, the combination of peptide length, a high positive charge and existence of hydrophobic amino acids allowing the formation of regular secondary structures make the peptides more prone to first interact with the plasma membrane components, and second, associate better with the membrane lipids, leading to a stronger membrane perturbation ability. Since RI-Tat is devoid of hydrophobic amino acids that could potentially affect the membrane stability, it is not considered a membrane active peptide (at least in the concentration range used in this study). We have observed an increased membrane interaction with all the longer more hydrophobic RI-peptides by the induction of intracellular PI staining (data not shown). The fact that even though strong PI staining was recorded but LDH leakage was not observed during treatment with the toxic RI-CPPs indicates that the RI-peptides do not damage the membrane to the extent that large molecules could pass through the damaged regions. Instead, local disturbances of the lipid bilayer may be induced leading to the entrance of the small PI molecules. Taken together, because of both the length and the high number of hydrophobic amino acid residues in their sequence, the used (longer and hydrophobic) RI-CPPs may also interact and destabilize the intracellular mitochondrial membranes, causing the observed loss in the mitochondrial potential (Fig. 5, Supplementary Fig. S6 and movie M2). However, due to the lack of further evidence, we cannot rule out the possibility that RI-CPPs act indirectly upon the mitochondrial potential and activity. Nevertheless, the maintenance of the transmembrane potential is required for most mitochondrial functions and under apoptotic conditions the gradual loss of the mitochondrial membrane potential causes a decline in the generation of ATP and ultimately leads to cell death [33]. Therefore, the RI-peptide-treatment negatively affecting the mitochondrial network gives further evidence for cytotoxic effects of the RI-modification and may possibly refer to a process of apoptosis. Our results illustrate that changes in the mitochondrial network are actually the first signs of

cytotoxic activity displayed by the longer hydrophobic RI-peptides (observed already after 15 min, Supplementary movie M2), indicating that this could be the initiator of the successive events.

To define if the cells underwent apoptotic events after RI-peptide treatment, their nuclear morphology was characterized by Hoechst staining. All three RI-peptides which reduced the cell viability, RI-Arf1-14, RI-M918 and RI-penetratin, affected the cell nuclei in the same range as staurosporine (Fig. 6). This method is not specific enough to be used as a single approach to determine the involvement of apoptosis, but it provides general information if and to what extent the nuclei are affected. A more specific approach is to measure the activation of caspases, such as caspase-3. 20 μM RI-penetratin induced a weak, but measurable, activation of caspase-3 in MDA MB 231 cells (Fig. 7). The same concentration of RI-Arf1-14, on the other hand, clearly activated caspase-3 in both MDA MB 231 and HeLa cells (Fig. 7 and Supplementary Fig. S7). Elevating the RI-penetratin concentration, however, induced the same extent of caspase-3 activation as observed in RI-Arf1-14-treated cells (Fig. 7). Thus, the mechanism behind the toxic effects of RI-penetratin and RI-Arf1-14 differs or, alternatively, RI-penetratin is a less potent apoptosis inducing peptide. RI-Arf1-14 induced the same morphological changes as RI-penetratin, but the effect was faster and more severe with diminished focal adhesions and mitochondrial network. The diminished mitochondrial potential and the strong activation of caspase-3 after RI-Arf1-14 treatment in both MDA MB 231 and HeLa cells indicate that this peptide is most likely inducing its effect through apoptosis. However, caspase-3 activation is not an absolute requisite for definite induction of apoptosis and several caspase-independent cell death processes have been described [33–35]. Therefore, although RI-penetratin at lower concentrations did not activate caspase-3, it could still induce apoptosis through disruption of the mitochondrial potential and the actin cytoskeleton.

In summary, we hypothesize that the loss of mitochondrial transmembrane potential by RI-peptides could trigger the cascade of cellular events leading to the subsequent reduction of metabolic activity, actin depolymerization, trypsin insensitivity, nuclear condensation and caspase-3 activation. To our knowledge, this is the first time adverse toxic effects evoked by RI-peptides are documented. The RI-isomerization has become a common way of increasing the stability of peptides, e.g. in the development of peptide vaccines and in the field of CPPs. Therefore, it is imperative that the adverse effects we have observed as a consequence of this modification become known.

Supplementary materials related to this article can be found online at doi:10.1016/j.bbamem.2010.10.019.

Acknowledgments

The work presented in this article was supported by Swedish Research Council (VR-NT); by Center for Biomembrane Research, Stockholm; by Knut and Alice Wallenberg's Foundation; by grants from Estonian Science Foundation (ESF 7058) and Estonian Ministry of Education and Research (0182691s05) and Sweden-Japan, Estonian COE. H. R. was supported by Olev and Talvi Maimets stipend and Artur Lind stipend fund.

References

[1] S. EL Andaloussi, T. Holm, Ü. Langel, Cell-penetrating peptides: mechanisms and applications, Curr. Pharm. Des. 11 (2005) 3597–3611.
[2] M. Mäe, S. EL Andaloussi, P. Lundin, N. Oskolkov, H.J. Johansson, P. Guterstam, Ü. Langel, A stearylated CPP for delivery of splice correcting oligonucleotides using a non-covalent co-incubation strategy, J. Control. Release 134 (2009) 221–227.
[3] J.S. Wadia, R.V. Stan, S.F. Dowdy, Transducible TAT-HA fusogenic peptide enhances escape of TAT-fusion proteins after lipid raft macropinocytosis, Nat. Med. 10 (2004) 310–315.
[4] P.A. Wender, D.J. Mitchell, K. Pattabiraman, E.T. Pelkey, L. Steinman, J.B. Rothbard, The design, synthesis, and evaluation of molecules that enable or enhance cellular uptake: peptoid molecular transporters, Proc. Natl Acad. Sci. USA 97 (2000) 13003–13008.
[5] D. Derossi, S. Calvet, A. Trembleau, A. Brunissen, G. Chassaing, A. Prochiantz, Cell internalization of the third helix of the Antennapedia homeodomain is receptor-independent, J. Biol. Chem. 271 (1996) 18188–18193.
[6] M. Chorev, M. Goodman, Recent developments in retro peptides and proteins—an ongoing topochemical exploration, Trends Biotechnol. 13 (1995) 438–445.
[7] M. Chorev, The partial retro-inverso modification: a road traveled together, Biopolymers 80 (2005) 67–84.
[8] P.M. Fischer, The design, synthesis and application of stereochemical and directional peptide isomers: a critical review, Curr. Protein Pept. Sci. 4 (2003) 339–356.
[9] C. Li, M. Pazgier, J. Li, C. Li, M. Liu, G. Zou, Z. Li, J. Chen, S.G. Tarasov, W.Y. Lu, W. Lu, Limitations of peptide retro-inverso isomerization in molecular mimicry, J. Biol. Chem. 285 (2010) 19572–19581.
[10] E.L. Snyder, B.R. Meade, C.C. Saenz, S.F. Dowdy, Treatment of terminal peritoneal carcinomatosis by a transducible p53-activating peptide, PLoS Biol. 2 (2004) E36.
[11] J. Brugidou, C. Legrand, J. Mery, A. Rabie, The retro-inverso form of a homeobox-derived short peptide is rapidly internalised by cultured neurones: a new basis for an efficient intracellular delivery system, Biochem. Biophys. Res. Commun. 214 (1995) 685–693.
[12] S. EL Andaloussi, H.J. Johansson, T. Holm, Ü. Langel, A novel cell-penetrating peptide, M918, for efficient delivery of proteins and peptide nucleic acids, Mol. Ther. 15 (2007) 1820–1826.
[13] H.J. Johansson, S. EL Andaloussi, T. Holm, M. Mäe, J. Jänes, T. Maimets, Ü. Langel, Characterization of a novel cytotoxic cell-penetrating peptide derived from p14ARF protein, Mol. Ther. 16 (2008) 115–123.
[14] S. EL Andaloussi, P. Guterstam, Ü. Langel, Assessing the delivery efficacy and internalization route of cell-penetrating peptides, Nat. Protoc. 2 (2007) 2043–2047.
[15] S.H. Kang, M.J. Cho, R. Kole, Up-regulation of luciferase gene expression with antisense oligonucleotides: implications and applications in functional assay development, Biochemistry 37 (1998) 6235–6239.
[16] C. Albiges-Rizo, O. Destaing, B. Fourcade, E. Planus, M.R. Block, Actin machinery and mechanosensitivity in invadopodia, podosomes and focal adhesions, J. Cell Sci. 122 (2009) 3037–3049.
[17] J.L. Vayssiere, P.X. Petit, Y. Risler, B. Mignotte, Commitment to apoptosis is associated with changes in mitochondrial biogenesis and activity in cell lines conditionally immortalized with simian virus 40, Proc. Natl Acad. Sci. USA 91 (1994) 11752–11756.
[18] A.G. Porter, R.U. Janicke, Emerging roles of caspase-3 in apoptosis, Cell Death Differ. 6 (1999) 99–104.
[19] H.J. Lee, W.M. Pardridge, Pharmacokinetics and delivery of tat and tat-protein conjugates to tissues in vivo, Bioconjug. Chem. 12 (2001) 995–999.
[20] Y.P. Jarajapu, J. Baltunis, H.J. Knot, S.M. Sullivan, Biological evaluation of penetration domain and killing domain peptides, J. Gene Med. 7 (2005) 908–917.
[21] D. Delaroche, F.X. Cantrelle, F. Subra, C. Van Heijenoort, E. Guittet, C.Y. Jiao, L. Blanchoin, G. Chassaing, S. Lavielle, C. Auclair, S. Sagan, Cell-penetrating peptides with intracellular actin remodeling activity in malignant fibroblasts, J. Biol. Chem. (2009).
[22] S. Etienne-Manneville, A. Hall, Rho GTPases in cell biology, Nature 420 (2002) 629–635.
[23] A.S. Maddox, K. Burridge, RhoA is required for cortical retraction and rigidity during mitotic cell rounding, J. Cell Biol. 160 (2003) 255–265.
[24] D.A. Starr, Communication between the cytoskeleton and the nuclear envelope to position the nucleus, Mol. Biosyst. 3 (2007) 583–589.
[25] S.S. Martin, P. Leder, Human MCF10A mammary epithelial cells undergo apoptosis following actin depolymerization that is independent of attachment and rescued by Bcl-2, Mol. Cell. Biol. 21 (2001) 6529–6536.
[26] D.J. Mitchell, D.T. Kim, L. Steinman, C.G. Fathman, J.B. Rothbard, Polyarginine enters cells more efficiently than other polycationic homopolymers, J. Pept. Res. 56 (2000) 318–325.
[27] U. Soomets, M. Lindgren, X. Gallet, M. Hällbrink, A. Elmquist, L. Balaspiri, M. Zorko, M. Pooga, R. Brasseur, Ü. Langel, Deletion analogues of transportan, Biochim. Biophys. Acta 1467 (2000) 165–176.
[28] A. Scheller, J. Oehlke, B. Wiesner, M. Dathe, E. Krause, M. Beyermann, M. Melzig, M. Bienert, Structural requirements for cellular uptake of alpha-helical amphipathic peptides, J. Pept. Sci. 5 (1999) 185–194.
[29] S. EL Andaloussi, P. Järver, H.J. Johansson, Ü. Langel, Cargo-dependent cytotoxicity and delivery efficacy of cell-penetrating peptides: a comparative study, Biochem. J. 407 (2007) 285–292.
[30] C.Y. Jiao, D. Delaroche, F. Burlina, I.D. Alves, G. Chassaing, S. Sagan, Translocation and endocytosis for cell-penetrating peptide internalization, J. Biol. Chem. 284 (2009) 33957–33965.
[31] S.W. Jones, R. Christison, K. Bundell, C.J. Voyce, S.M. Brockbank, P. Newham, M.A. Lindsay, Characterisation of cell-penetrating peptide-mediated peptide delivery, Br. J. Pharmacol. 145 (2005) 1093–1102.
[32] J. Mueller, I. Kretzschmar, R. Volkmer, P. Boisguerin, Comparison of cellular uptake using 22 CPPs in 4 different cell lines, Bioconjug. Chem. 19 (2008) 2363–2374.
[33] S.W. Tait, D.R. Green, Caspase-independent cell death: leaving the set without the final cut, Oncogene 27 (2008) 6452–6461.
[34] N.J. McCarthy, M.K. Whyte, C.S. Gilbert, G.I. Evan, Inhibition of Ced-3/ICE-related proteases does not prevent cell death induced by oncogenes, DNA damage, or the Bcl-2 homologue Bak, J. Cell Biol. 136 (1997) 215–227.
[35] J. Xiang, D.T. Chao, S.J. Korsmeyer, BAX-induced cell death may not require interleukin 1 beta-converting enzyme-like proteases, Proc. Natl Acad. Sci. USA 93 (1996) 14559–14563.
[36] A. Elmquist, Ü. Langel, In vitro uptake and stability study of pVEC and its all-D analog, Biol. Chem. 384 (2003) 387–393.